Design and test of a gripper prototype for horticulture products

RUSSO, Matteo, CECCARELLI, Marco, CORVES, Burkhard, HÜSING, Mathias, LORENZ, Michael, CAFOLLA, Daniele and CARBONE, Giuseppe <http://orcid.org/0000-0003-0831-8358>

Published version

RUSSO, Matteo, CECCARELLI, Marco, CORVES, Burkhard, HÜSING, Mathias, LORENZ, Michael, CAFOLLA, Daniele and CARBONE, Giuseppe (2016). Design and test of a gripper prototype for horticulture products. Robotics and Computer-Integrated Manufacturing, 44, 266-275.

Design and Test of a Gripper Prototype for Horticulture Products

Matteo Russo[1], Marco Ceccarelli[1], Burkhard Corves[2],
Mathias Hüsing[2], Michael Lorenz[2], Daniele Cafolla[1], Giuseppe Carbone[1]

[1] LARM: Laboratory of Robotics and Mechatronics – DiCEM
University of Cassino and Southern Latium
Via di Biasio 43 – 03042 Cassino (FR), Italy
{matteo.russo, ceccarelli, cafolla, carbone}@unicas.it

[2] IGM: Institut für Getriebetechnik und Maschinendynamik
Rheinisch-Westfälischen Technische Hochschule – RWTH Aachen
Kackertstraße 16-18 – 52072 Aachen, Germany
{lorenz, corves, huesing}@igm.rwth-aachen.de

Abstract: This paper describes the design of a gripper for horticulture product grasping. The design solution has been achieved by means of a systematic approach by evaluating all the possible architecture. The proposed structure is optimized and numerically simulated. Then, a prototype has been built and tested in laboratory. The design process and test results are discussed to show the efficiency of the built prototype with lab tests.

Keywords: Robot Design, Grasping, Horticulture Products, Grippers, Experimental Mechanics

1 Introduction

The end-effector can be considered the most important component of a robot when it deals with horticulture products, since it acts as interface between the robotic system and product. Since fruits and vegetables usually have irregular changeful shapes and low mechanical properties, the end-effector must be designed properly to grasp them. Robotics applied to horticulture products handling has been studied for more than twenty years. However, research results have been focused on single-product applications and end-effectors have been designed only for specific targets [1], such as tomatoes [2][3][4], strawberries [5] and cucumbers [6]. In particular, [2] describes the design process and the prototyping of a gripper for tomato harvesting. In [3], the mechanical properties of tomatoes while grasped by robotic fingers are analyzed by measuring maximum deformation for different grasp conditions at collision status. In [4] a packaging system for tomatoes with underactuated fingers is presented, while a gripper for strawberry harvesting is introduced in [5] and [6] describes the development of an autonomous robot for cucumbers harvesting. Those experiences show that current

grippers are specifically designed for a single application and they are not flexible enough to adapt to a wide variety of shapes and sizes.

An important challenge to improve grippers can be recognized in the use of compliant components. They are non-rigid materials that are able to adapt passively to the irregular shape of horticulture products. Furthermore, compliance increases contact surfaces and reduces the stress on grasped objects. Even if an end-effector with compliant elements is not a universal gripper for all horticulture products, it can deal with a wide variety of objects in a wide range of shapes and dimensions. The MultiChoiceGripper, shown in [7], is an example of compliant gripper.

This paper presents the development of an end-effector that is able to grasp medium-sized spherical fruits. This gripper shows suitable functioning for careful grasp and release of horticulture products. In Section 2, horticulture products are analyzed to identify the requirements for a suitable gripper. In Section 3 the chosen structure is described, and then its mechanical design is optimized and elaborated for rapid prototyping. Section 4 presents the experimental tests made with the built prototype. Finally, Section 5 contains conclusive remarks on this work and possible future developments.

2 Requirements for Horticulture Products Handling

Nowadays, the harvesting of horticulture products is usually performed manually by workers. Post-harvesting operations are usually executed by automatic selection and packaging lines, as shown in Figure 1a. However, packaging for high-quality products are still performed mostly by human operators, as shown in Figure 1b. The main obstacle to an automatization of the task is the efficiency of grippers, since a gripper should be able to carefully grasp and hold horticulture products. This can lead to lower production costs and to decrease the lead time between the harvest and market sale.
In order to design a gripper for a robotic unit, object analysis is required [8]. This paper deals with medium-sized horticulture products, such as apples, tomatoes, citrus fruits and peaches. Since 1961, the Organization for Economic Co-operation and Development (OECD) sets international standards for fruits and vegetables, with information about the standard dimensions for commercial products [9]. Relevant information is summarized in table 1. The OECD sets standards, even for the quality of fruits and vegetables, but a scientific approach is not used for quality checks, since only a visual observation is required for quality parameters [9]. The average diameter of most of the considered horticulture products is in the range of 40 to 100 mm. Weight varies even within species, but it is always in the range of 50 to 500 g [9]. The shape of those products is approximately spherical with some notable exceptions in lemons and oblong tomatoes. The mechanical properties of apples, pears and tomatoes were measured in several research projects [10][11][12]. Data are summarized in table 2. Since a tomato has the worst mechanical properties, it can be used as a reference fruit for the design of grippers for horticulture products.

a) b)

Fig. 1. Examples of packaging lines: a) Automatic packaging line for apples; b) Packaging operations performed by human workers.

Table 1. Sizes of horticulture products as from standards in [9].

Product:	Min. size [mm]:	Max. size [mm]:
Apples	60	110
Apricots	30	60
Clementines	35	60
Lemons	45	90
Oranges	53	120
Peaches	56	100
Tomatoes	35	105

Table 2. Mechanical properties of common fruits and vegetables [10][11][12].

Product:	Young's Modulus average [MPa]	Young's Modulus deviation [MPa]	Poisson's Ratio [-]
Tomato – Ripe	2.32	N.A.	0.74
Tomato – Unripe	4.07	N.A.	0.55
Pear	5.80	0.50	0.25
Apple	12.89	2.43	0.32

Possible end-effector solutions can be identified through general considerations among the following architectures, as summarized in table 3:

- Grippers, which are composed by two or more rigid fingers and a mechanism to move them against an object. A gripper usually has a 1 to 3 degrees-of-freedom structure. Force control is essential for functioning and even a single sensor is enough to avoid damaging the object. The low flexibility of a gripper is its main disadvantage, since rigid fingers cannot wrap around an object or adapt to it.
- Artificial hands, whose design makes them similar to a human hand. They are composed of multiple anthropomorphic fingers and they are capable to close them onto an object by wrapping around it. They can be flexible and adapt to most shapes,

but they need several actuators and sensors. This makes the control complex and leads to excessive costs.

- Pneumatic devices, which use partial vacuum to lift objects with non-porous surface. The grasp is difficult to control and it can leave traces on the surface of horticulture products or even damage them. In addition, suction cups could not adhere to some curved or irregular surfaces, failing to pick the product up. For those reasons, pneumatic devices cannot be considered suitable for applications with horticulture products.
- Other end-effectors, which can be based on magneto- or electro-adhesion; they are not able to manage organic products.

Thus, a suitable end-effector design can be considered as a crossover of grippers and hands, since it should be flexible to adapt even to irregular shapes but at the same time it should have a structure with 1 to 3 DoF for an easy control.

Table 3. Requirements for end-effectors in the grasp of horticulture products.

Requirement	Gripper	Hand	Pneum. Devices
Geometry:			
Radius: 20-50 mm	Yes	Yes	Yes
Forces:			
Firm grasp	Yes	Yes	No
No damage	Yes	Yes	No
Energy:			
Electric drives	Yes	Yes	No
Materials:			
Non-toxic material	Yes	Yes	Yes
Operation:			
Easy to control	Yes	No	Yes

The most important component of a robotic gripper or hand is the finger, since it is the part that directly contacts the grasped object. The finger design can be approached by using the following solutions:

- Rigid fingers, consisting of a single rigid body; they are moved by the end-effector's mechanism. They achieve grasp also through friction. Most of the current gripper designs use them since they are fairly easy to design, build and control.
- Articulated fingers, which are formed by two or more bodies connected by actuated joints. They can adapt their grasp configuration to irregular and complex shapes but they require a more elaborated design and a control with multiple motors.
- Compliant fingers, which are based on compliant materials. This finger design has a structure that can adapt to irregular shapes. Compliance increases contact surface, therefore decreasing stresses on the grasped object.

Table 4 summarizes the performance expectations of the above solutions. After evaluating those aspects, a 1-DoF gripper with compliant fingers has been selected as a suitable design for the grasp of horticulture products.

Table 4. Requirements for finger structure in the grasp of horticulture products.

Requirement	Rigid Finger	Articulated Finger	Compliant Finger
Forces:			
Firm grasp	Yes	Yes	Yes
No damage	Yes	Yes	Yes
Adaptive	No	Yes	Yes
Materials:			
Non-toxic material	Yes	Yes	Yes
Operation:			
Easy to control	Yes	No	Yes

3 Gripper Design

The design of the proposed gripper has been developed by means of a systematic procedure that has been outlined by Pahl and Beitz [8], in accordance to VDI guideline. The design process has been approached with a specific attention to an application for horticulture products by following the steps in Fig. 2:

- Problem analysis for task description and identification;
- Definition of task requirements;
- Conceptual design based on function structures;
- Evaluation on technical and economic efficiency;
- Development of a preliminary design;
- Optimization of size and functionality;
- Definitive design and CAD model.

The task requirements have been analyzed in details as reported in section 2 with reference to OECD standards [9], in order to identify the main characteristics both for design and operation purposes. The structure of the gripper has been selected by analyzing the required functionalities for horticulture products in order to get a linkage solution with proper grasp mechanics. The definitive design is developed with specific drawings of the parts, after an iterative optimization process.

The proposed solution is a three-fingered gripper that is based on the crank-slider mechanism as in Figure 3a. The finger (body 2) is connected to a rocker (body 1) and to the slider (body 3). The sliders of the three fingers are fixed to the same frame and their motion is controlled by a single linear actuator. Even if high-compliance fingers can be used, a rigid mechanism can be preferred, since it is fairly easy to analyze, to build and to test for a proper grasping operation. Compliance is restrained to the fingertip region. The most important parameter of fingertips is the material, since it has to have a hyper-elastic behavior. A possible solution can be identified with a kind of rubber. Several different rubbers can be used for the grasping application, such as the following ones:

- Foam rubber, which is a rubber that is manufactured with a foaming agent to create an air-filled matrix structure [13]. It is usually made of either polyurethane or latex,

so that it is lightweight and it can dampen impacts, cushioning the product during the manipulation, but its friction coefficient could be too low for the task.

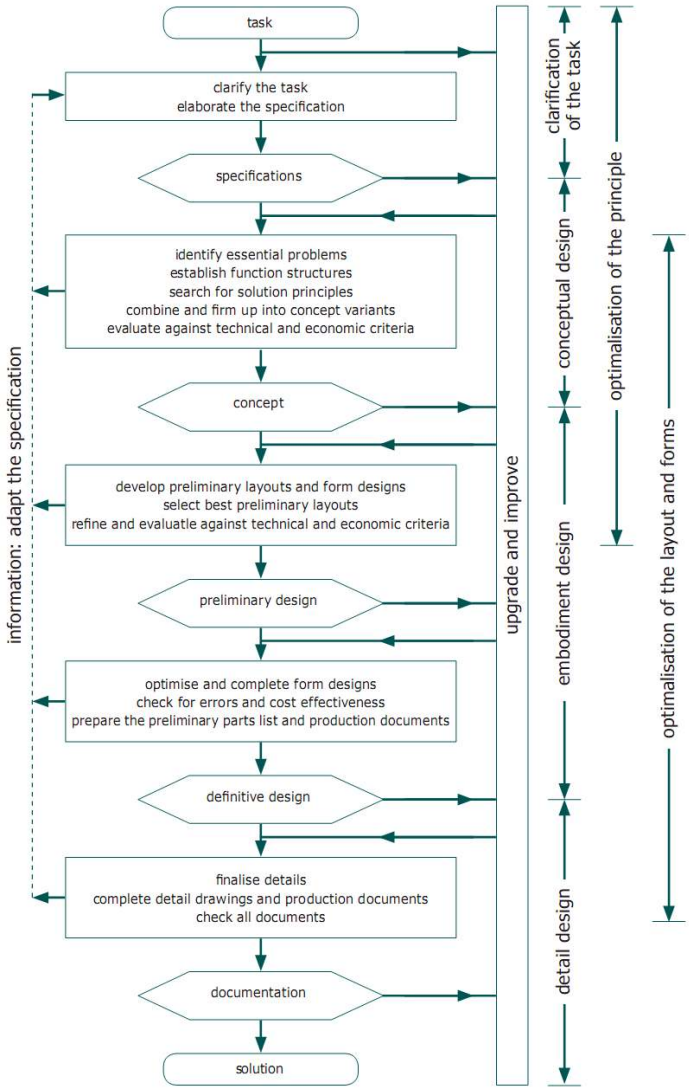

Fig. 2. Procedure for systematic engineering design in accordance with VDI guideline 2221 [8].

- Natural rubbers, which are based on latex and are harvested from certain trees [13]. They have a large stretch ratio and high resilience.
- Silicone rubber, a stable and resistant elastomer. It can be easily shaped in its gel or liquid state through injection molding and then it can be converted into its solid state

through a post-injection process. It is highly inert, but its impact-dampening capacity can be lower than foam rubbers [13].
- Other synthetic rubbers, which can be used as long as they do not contain toxic plasticizers such as phthalates.

Among all the possible choices, the Grasping Index (*G.I.*) in [14] is used as design criterion, since it is a compact expression to evaluate the performance of a gripper mechanism. The Grasping Index is defined by [14] as

$$G.I. = \frac{F \sin \zeta}{P} \tag{1}$$

in which P is the force exerted by the actuator, F the grasping force and ζ represents the configuration angle of the mechanism at grasp. The following equations can be written with reference to the design parameters shown in Figure 3b to describe the kinematics of the gripper mechanism as

$$l_2 \sin \psi = l_1 \sin \phi \tag{2}$$

$$\cos \phi = \frac{x_B{}^2 + l_1{}^2 - l_2{}^2}{2 x_B l_1} \tag{3}$$

where l_1 and l_2 are respectively the length of the first and second link of the mechanism and the position of the slider x_B describes the configuration of the mechanism.
In addition, static grasp equilibrium can be evaluated to characterize mechanism performance at grasp. With reference to Figure 3c, the equilibrium conditions for moments around point B and for forces in X-direction can be written as

$$Fh - R_{12t} l_2 = 0 \tag{4}$$

$$R_{12x} - P = 0 \tag{5}$$

where forces R_{12x} and R_{12t} represent the component of constraint reaction R_{12} respectively along X-axis and the axis normal to link 2 (AB). Since no external force or moment acts on link 1 (A_0A), R_{12} shares the same orientation ϕ of that link. Reactions R_{12x} and R_{12t} can be expressed as

$$R_{12t} = R_{12} \cos\left(\phi + \psi - \frac{\pi}{2}\right) \tag{6}$$

$$R_{12x} = R_{12} \cos \phi \tag{7}$$

These equations give

$$P = \frac{Fh \cos \phi}{l_2 \cos\left(\phi + \psi - \frac{\pi}{2}\right)} \tag{8}$$

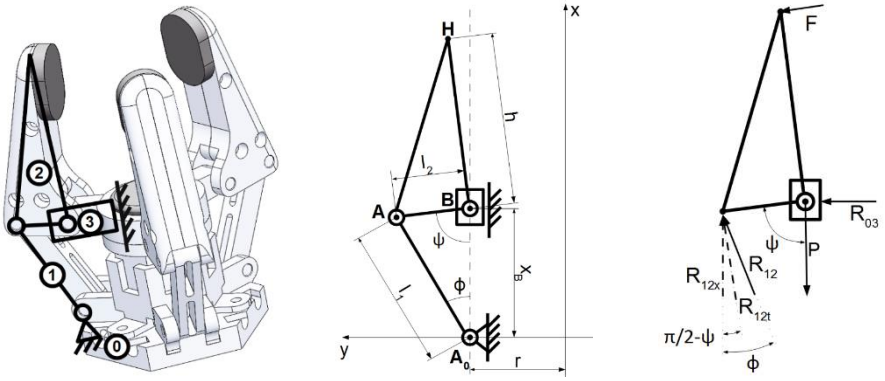

a) b) c)

Fig. 3. The proposed gripper solution: a) kinematic scheme of the finger mechanism; b) Kinematic diagram with design parameters; c) Free-body diagram for finger (body 2) and slider (body 3).

Then, substituting Eqs. (2) and (8) in Eq. (1), the Grasping Index for the proposed gripper can be expressed as

$$G.I. = \frac{l_1}{h} tg\, \phi \cos\left(\phi + \psi - \frac{\pi}{2}\right) \tag{9}$$

As shown in Eq. (9), the *G.I.* of the gripper depends on the ratio of the first link to the height of the finger and on the mechanism configuration. The easiest way to increase the Grasping Index is to make the finger as short as possible decreasing finger height h. Unfortunately, the minimum height is constrained by the dimension of the product since it must be more than half the maximum diameter of the grasped object. The other direct dependence of the *G.I.* is on l_1. Since l_1 has influence even over the configuration-dependent part, any change could result into unexpected variations of the *G.I.*. Therefore, no trivial optimization is possible and a numerical optimization through the solution of an optimization problem is required, since the Grasping Index is configuration-dependent. Thus, the mechanism can be optimized in two different ways [14], namely:

- Maximizing the Mean Grasping Index, that can be expressed as

$$max\ G.I._{mean}\ \ subject\ to\ l_{i,min} < l_i < l_{i,max}\ for\ i = 1,2 \tag{10}$$

- Minimizing Grasping Index deviation, by using as problem formulation

$$min \frac{G.I._{max} - G.I._{min}}{G.I._{mean}}\ subject\ to\ l_{i,min} < l_i < l_{i,max}\ for\ i = 1,2 \tag{11}$$

Each geometrical parameter of the gripper is constrained between a minimum dimension and a maximum one as related to the given product range, as shown in table 5. Smaller links make hinge manufacturing and assembling difficult. Bigger links results in a gripper that is over dimensioned for the task. In order to get the optimal

values of the design parameters of the gripper, their ranges have been discretized and the *G.I.* has been evaluated for each possible combination of geometry. Then, for each geometry, the mean *G.I.* and the *G.I.* deviation have been evaluated for all the configurations. Optimization results are shown in table 6.

Table 5. Limits of ranges of design parameters of the gripper.

Variable:	Min. [mm]:	Max. [mm]:
l_1	30.00	60.00
l_2	15.00	20.00
r	30.00	30.00

Table 6. Results of gripper optimization.

l_1 [mm]	l_2 [mm]	$G.I._{mean}$	Deviation:	Criterion:
30.00	20.00	0.316308	0.126631	Max. Mean G.I.
42.00	20.00	0.297702	0.060774	Min. Deviation

Since the first solution looks better than the second one in terms of the mean *G.I.* (6.2%) but significantly worse (108.5%) in deviation, the one with minimum deviation can be considered the most convenient. The chosen design solution refers to the case with l_1 equal to 42.00 mm and l_2 equal to 20.00 mm. The stroke of the slider for that solution is 15.00 mm, with x_B ranging from 31.00 to 46.00 mm. The distance of the fingertip from the axis of symmetry, as in Figure 3b, is equal to the mean radius of the grasped product and can be expressed as

$$r_H = r + h\,sin\left(\frac{\pi}{2} - \psi\right) \tag{12}$$

By analyzing the gripper motion with the designed mechanism structure, r_H ranges from 7.25 mm to 58.61 mm. Therefore, the gripper is able to grasp any product within a diameter range of 14.50 to 117.22 mm. Actuation force P can be evaluated from Eq. 8 by using force F, mechanism geometry, and mechanism configuration. Once configuration of the gripper is determined from its kinematics, the force F can be calculated by using the static equilibrium conditions at grasp. The following assumptions refer to the facts that both fingers and product are modeled as rigid bodies and there are no external forces. The Coulomb model, with friction coefficient μ equal to 0.5, can conveniently describe friction between finger and product. Each finger is loaded in the same way (as for an axial-symmetric condition) with payload Q. Thus, from Figure 3c, the balance of forces on Z-axis can be written as

$$3\mu F\,sin\,\psi - 3F\,cos\,\psi - Q = 0 \tag{13}$$

to give

$$F = \frac{Q}{3(\mu\,sin\,\psi - cos\,\psi)} \tag{14}$$

By substituting Eq. 14 into Eq. 4, the maximum actuation force P_{max} can be computed straightforward. Most horticulture products have a weight that ranges between 0.5 and 2.0 N [9]. By assuming a product weight of 5.0 N with a design factor of safety equal to 2.5, P_{max} is computed as equal to 106.66 N, while the mean actuation force P_{mean} between all the configurations is equal to 56.41 N. A rotational motor – such as a stepper or servo DC motor – can be conveniently used to actuate the gripper by adding a lead screw in the system. In order to compute the actuation torque, the screw geometry needs to be modeled. A commercial spindle and lead screw nut have been chosen to gather data [15] and later to build a prototype. The spindle and the nut are trapezoidal-threaded (DIN103 Tr.10x3). The torque required to raise a load with a lead screw is given by [16] as

$$T = \frac{P d_m}{2}\left(\frac{l+\pi\mu_s d_m}{\pi d_m+\mu_s l}\right) \tag{15}$$

where l is the lead of the screw, d_m its mean diameter and μ_s the friction coefficient for the sliding contact between screw and nut. Static friction coefficient is $\mu_s = 0.33$ for dry steel nut on steel screw and dynamic dry friction coefficient is $\mu_{sd} = 0.15$, as reported in [15]. Maximum required torque is then computed as $T = 0.22$ Nm.
The gripper design has been completed through a 3D CAD model with all the details. The CAD model of the gripper is based on the above-mentioned results and it is aimed at 3D printing of a prototype [17]. Even if the assembly can be assembled using only 8 bodies – mechanism base, three rockers, three fingers, slider – it is actually composed by 23 components, since many bodies have been split into two or three parts for a proper mechanical design. This split is due to two different reasons: first of all, it allows for better material management in 3D printing manufacturing process by decreasing waste material; then, it makes hinge printing easier. Figure 4 shows the final CAD assembly of the mechanical design.

4 Prototype and Experimental Tests

A prototype has been built by using 3D printing manufacturing to check the feasibility of the construction. The gripper has been equipped with a RB350018-2AH22R gear motor as actuator [18] and is installable on the serial robotic arm UR5 by Universal Robots [19]. The designed gripper has been built through a Stratasys Dimension Elite 3D Printer [20]. The Dimension Elite Printer is able to print objects up to 200x200x300 mm with a layer thickness equal to 0.254 mm. The material that was used by the printer is ABS+ plastic. Even if it is possible to print assembled hinges with this technology, separate printing and later assembly of components has been chosen to limit errors and to have the possibility to replace misprinted or damaged components without replacing the entire structure. The compliant parts were made out of Polyurethane foam rubber by using a layer with thickness equal to 10 mm. The printed prototype is shown in Figure 5.

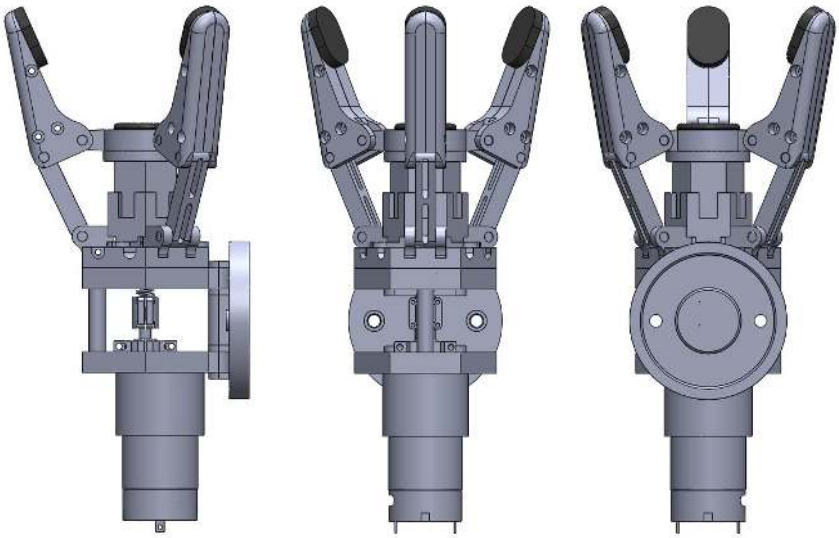

a) b) c)

Fig. 4. A final CAD design of the gripper: a) Right view; b) Front view; c) Rear view.

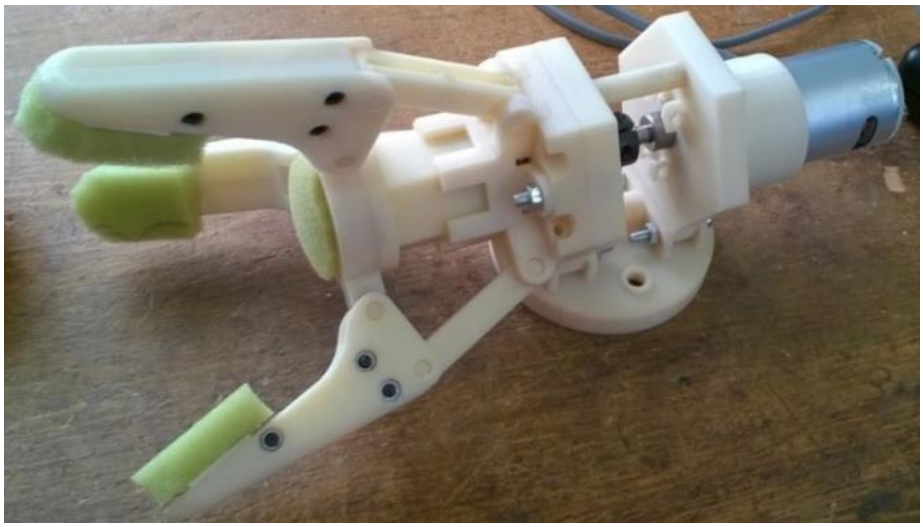

Fig. 5. The gripper prototype built with 3D printing.

Electric switches have been used to keep the control as simple as possible: they send a signal when the trigger is below a critical position. Three different switches are used to send the following signals:

- A fingertip switch is installed to stop the motor at the grasp operation. It is encased in fingers as shown in Figure 6a and 6b, beneath the compliant part of the fingertip. It triggers only over a certain deformation of the component.

a) b) c)

Fig. 6. Finger switches encased in the hand structure: a) A CAD model of the fingertip switch; b) The prototype installation for the fingertip switch; c) A CAD model of the fingerbase switch.

- A security stop switch is needed to stop the grasp if the gripper close command is given while there is no object between fingers. The security stop switch is triggered for any configuration in which the fingertips are near to collide to each other. Without this trigger, the motor would go on, and collisions could occur between the fingers. These collisions could damage the gripper and/or the lead screw transmission.
- A fingerbase switch is needed to stop the motor after a gripper open command. The switch is triggered for a critical relative position of rocker and finger, as shown in Figure 6c.

Operation control has been performed through robot UR5 user's interface [19], which allows to plan the motion of the robot by giving way points and predetermined commands triggered by input signals.
The gripper prototype has been tested in several different pick and place operations, with different products (ripe tomatoes, unripe tomatoes, peaches, apples). Each test is composed of three to ten basic pick&place tasks. The tested pick&place task for a single product is described in table 7 by using elementary action decomposition for operation planning. An elementary action is defined as the smallest manipulative entity that can be performed by the simplest action of the actuation in a robotic system through a single programming instruction. Elementary actions are detected and classified as transport (T), movement (M), active pause (A) and passive pause (P) [14]. Once all the elementary actions have been identified, they can be organized for a suitable and efficient manipulation sequence. Furthermore, they allow to easily identify programming instructions. The layout of the testing environment is shown in Figure 7.

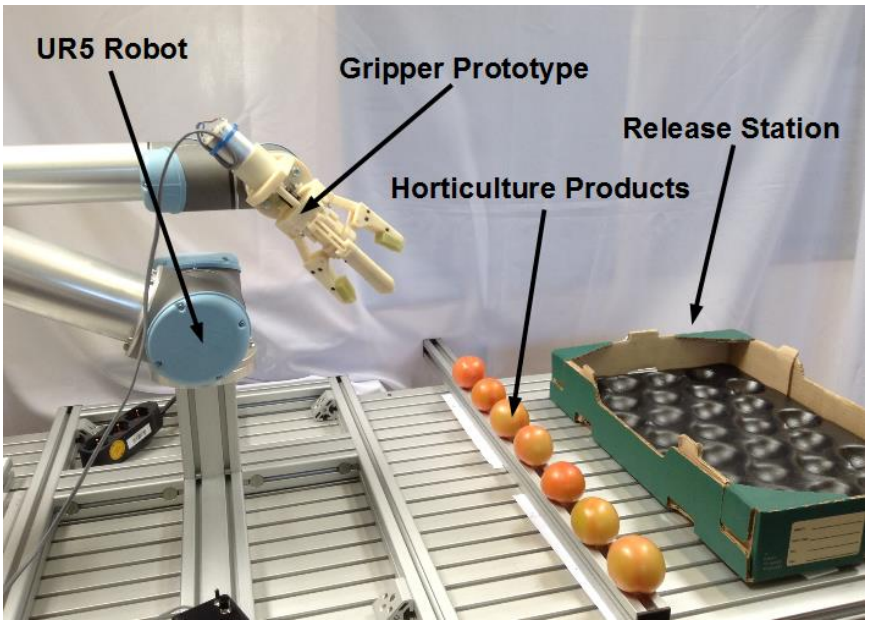

Fig. 7. Laboratory layout of the testing environment.

During the tests, each product has been lifted from the initial position, transported onto a socket of the final package and released into it. Furthermore, another test has checked the stability of the grasp: the robot grasps a tomato and moves it along a given path at its maximum speed (1.0 m/s) to check if grasp holds firmly.
During the tests, none of the horticulture products has been damaged by the manipulation shown in Figure 8, as a visual inspection of the manipulated object did not detect any pressure mark nor cracks. The firm grasp does not allow relative motion between horticulture products and fingers. The full cycle time for a single pick&place task is 2.0 seconds for a maximum path of 1.0 m, while the maximum actuation torque of the gripper is equal to 0.098 Nm.

Table 7. Elementary actions analysis [14] for the pick&place task of laboratory tests.

PICK&PLACE TASK	**T**	**M**	**A**	**P**
Manipulator moves onto grasping position		X		
The product is grasped			X	
Manipulator lifts up the object	X			
Manipulator moves onto release point	X			
Manipulator goes down to first release position	X			
The object is released			X	

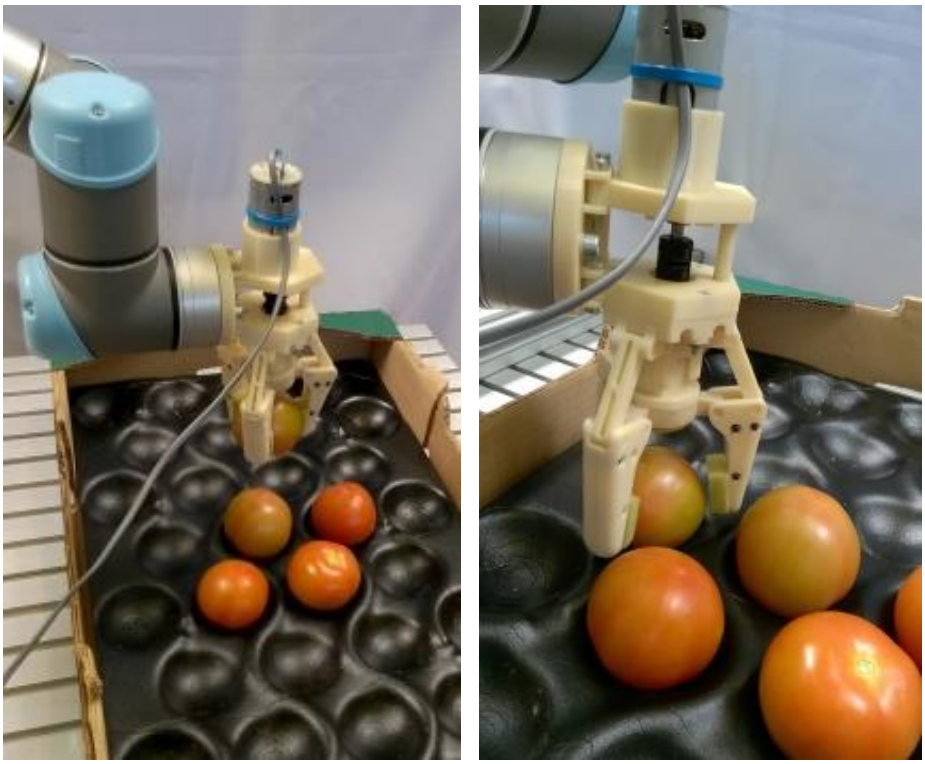

a) b)

Fig. 8. Main elementary actions in Table 6 for a laboratory test with tomato: a) Transport (T); b) Release action (A).

In order to measure the grasping force, other tests have been performed by using three Force Sensitive Resistors (FSR), which return a voltage that is related to the force that acts onto their sensing surface. The sensors have been placed between the rigid and the compliant part of the fingers. The scheme in Fig. 9 shows the data acquisition system setup. The system is composed by the three FSR sensors [21] that are connected to an Arduino Nano [22] and by three 10 kΩ stepdown resistances. In order to measure the power absorbed by motor, an ACS 712 current module [23] has been connected in series to the 6V power supply.

Several tests have performed in the laboratory, with the gripper grasping three different objects: a tennis ball, shown in Fig. 10a-b and used as reference, an unripe tomato and a ripe tomato, as in Fig 10c-d. For each object, static grasping tests and tests with robot motion have been repeated 24 times. The grasping tests with robot motions are characterized like the static ones, since it has been observed in the experimental tests that for maximum test velocity (2 m/s) there are no significant differences between static and dynamic results, as recorded through the FSR sensors on the fingers.

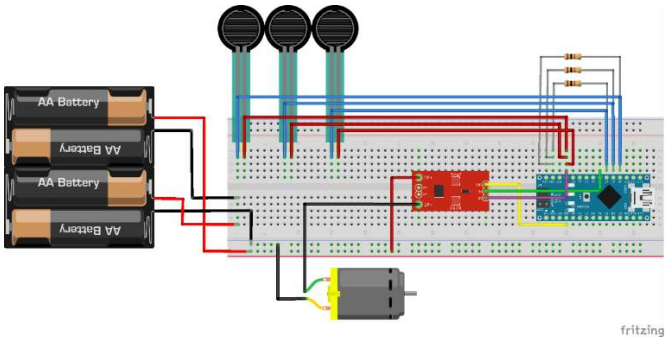

Fig. 9. Layout of the data acquisition system for the measure of grasping force and power consumption.

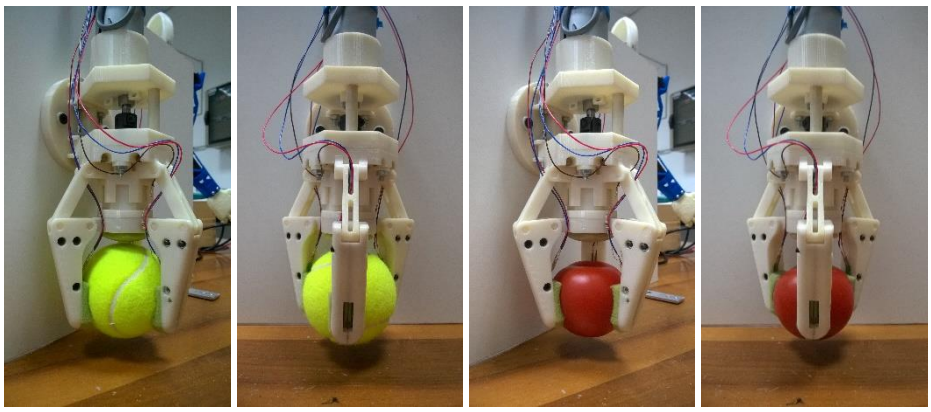

a) b) c) d)

Fig. 10. Test configuration for static grasping force measurement: a) Tennis ball, side view; b) Tennis ball, front view; c) Ripe tomato, side view; d) Ripe tomato, front view.

Fig. 11-16 show the results of tested grasps for the above-mentioned objects with four different plots: three represent the time evolution of the grasping force as measured by each sensor, while the fourth shows the power consumption that is obtained through the multiplication of the current measured by the 6V voltage of the power supply. The time has been taken from the internal clock of Arduino Nano and it is measured in milliseconds.

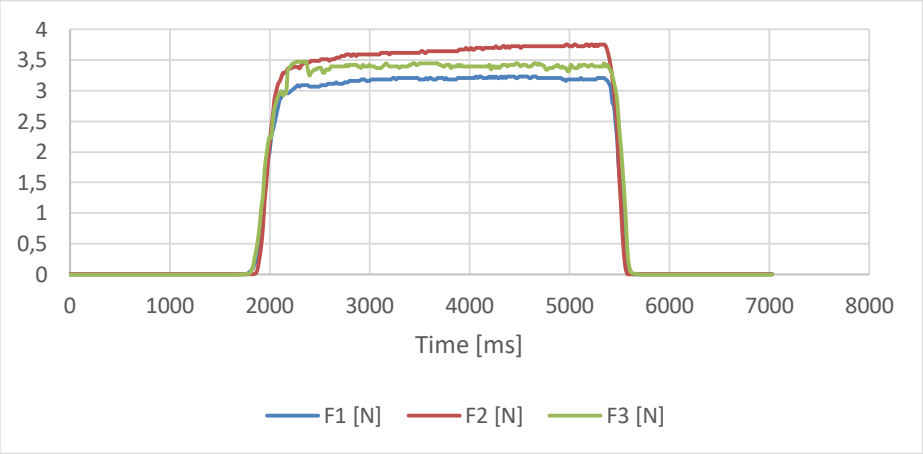

Fig. 11. Test results for grasping force measured by the FSR sensors for the tennis ball.

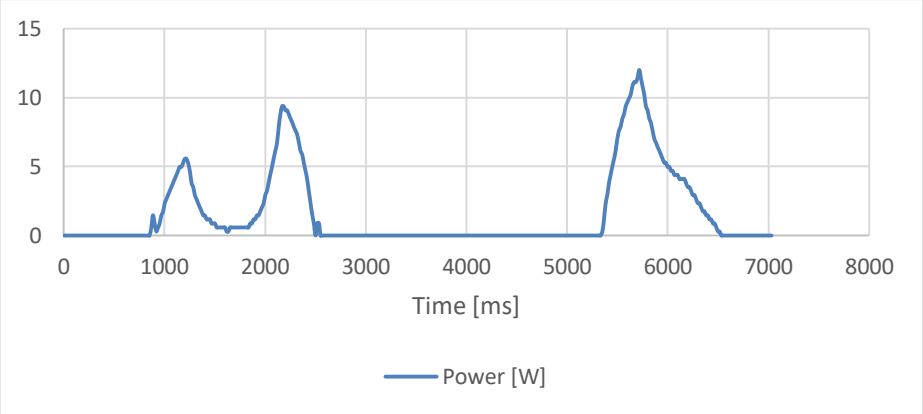

Fig. 12. Test results for power consumption [W] for the tennis ball.

The results for the grasping test of the tennis ball shown in Fig. 10a-b are shown in Fig. 11 and Fig. 12. As shown in Fig. 11, the shape of the function representing the measured force is approximately a square wave, since the force rises to its maximum within 0.1 s from the impact of the object against the finger and decreases to 0 N in a similar time during the release action. Therefore, the value of the force is approximatively constant during the grasp and its mean value is equal to 3.12 N (Fig. 11). Power consumption is characterized by three peaks, as shown in Fig. 12: the first one when the gripper begins to close, the second at the end of the grasping action when the stop switch is triggered, and the last one when the gripper releases the object. The maximum power consumption measured is 12.1 W.

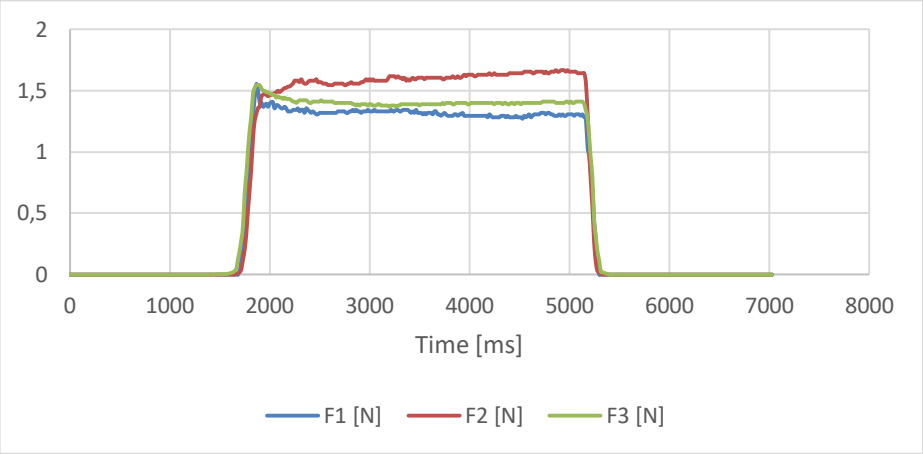

Fig. 13. Test results for grasping force measured by the FSR sensors for the unripe tomato.

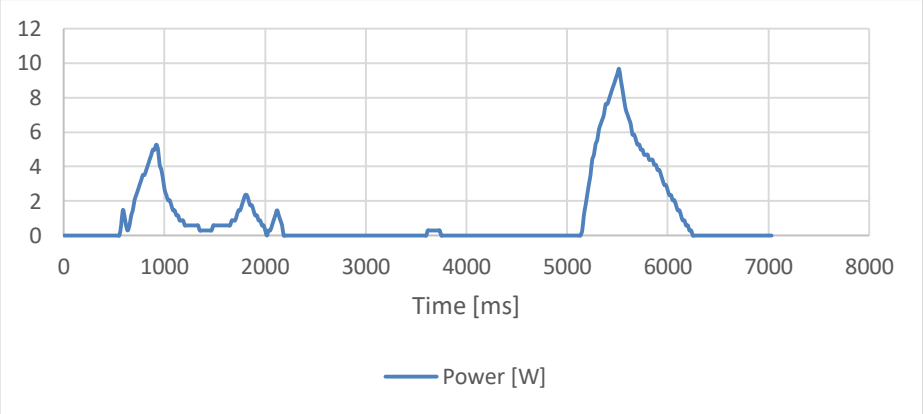

Fig. 14. Test results for power consumption [W] for the unripe tomato.

Fig. 13 shows the evolution of the grasping force during the grasp test on the unripe tomato. The shape of the function is again approximable to a square wave with a mean force at grasp equal to 1.42 N. The evolution of power consumption is shown in Fig. 14 and is similar to the one in Fig. 12, with a maximum power consumption equal to 9.8 W in the release peak.

The results of the test with the ripe tomato are comparable to the others and the same remarks apply. The mean force at grasp, as in Fig. 15, is equal to 0.88 N, while the maximum power consumption, shown in Fig. 16, is again in the release action and it is equal to 9.8 W.

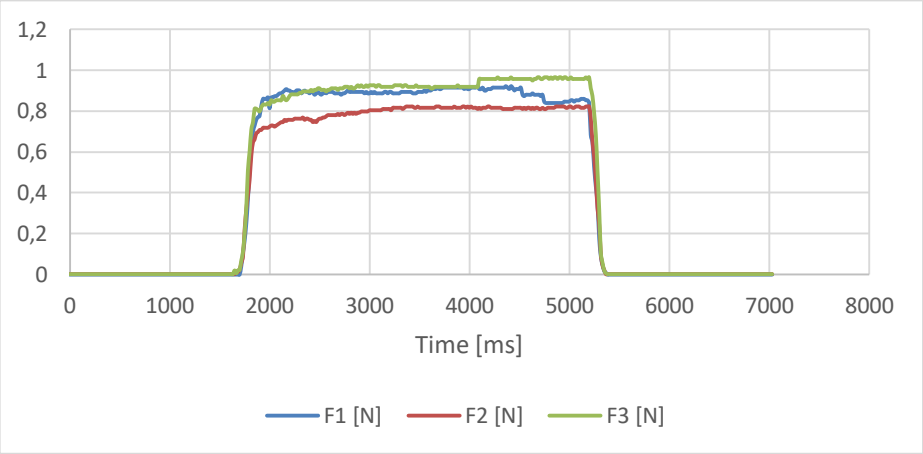

Fig. 15. Test results for grasping force measured by the FSR sensors for the ripe tomato.

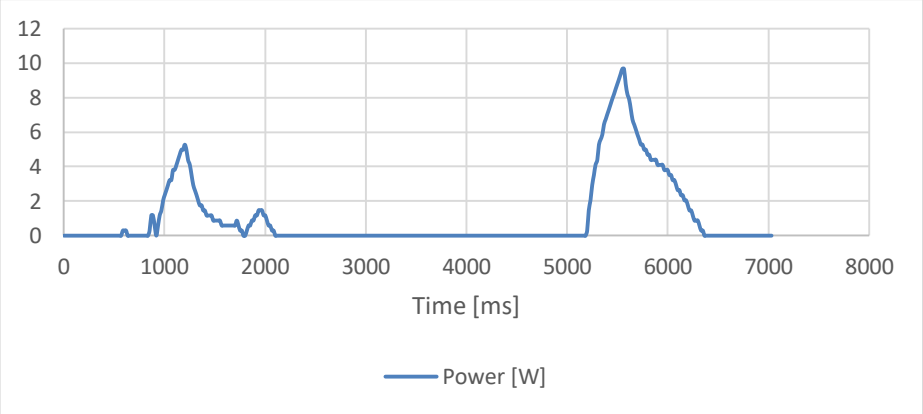

Fig. 16. Test results for power consumption [W] for the ripe tomato.

The time evolution of both grasping force and power consumption is similar in all the performed tests. The energy demand is similar for the three objects. Therefore, it depends on the kind of motion and is only marginally influenced by the applied grasping force. The contact is not characterized by a force peak as it happens in rigid grippers, since the foam fingertips successfully dampen the impact. A difference between the values that are measured by the three sensors in each test can be detected. This difference is caused by several factors that can be identified mainly in:

- Irregularities in the shape of the grasped objects;
- Inaccurate positioning of the gripper to grasp the product;
- Presence of noise in the acquired signals;
- Low accuracy and fixed position of the FSR sensors.

Furthermore, a difference in the grasping force values between the three products can be detected. This difference can be considered as due to many aspects (size, ripeness,

surface conditions and so on), but the performed tests stressed the influence of the compliance of the grasped object, since for higher product compliance the grasping force has been measured as lower. The possible reasons for this behavior are two, namely sensor capacity and product status. The first one is related to the FSR nature, that gives a force and not a pressure as a result. Therefore, since for the most compliant objects the pressure is spread onto a larger surface and it could reach the geometrical limits of the FSR, the measured force could result as lower than it actually is. The second reason is linked to the deformation of product and fingertip, since the measured force depends on the deformation of the fingertip but not on the deformation of the grasped object. Thus, the measured force in the grasp of a tennis ball or a ripe/unripe tomato is different even when the size is the same because the tomato is able to store more strain energy than the tennis ball.

5 Conclusions

In this paper, a new gripper for horticulture products is proposed as result of a specific design procedure by considering requirements and peculiarities for the grasp of horticulture products. Its kinematics has been studied and the mechanism has been optimized through results of numerical simulations. The gripper design has been modelled for prototyping through 3D printing manufacturing. The prototype has been tested by using a UR5 robot arm in several pick&place operations to demonstrate that the proposed gripper is able to fulfil all requirements for the task. It grasps firmly medium-sized horticulture products without damaging them. Future developments include an optimization of the compliant component of the fingertips and better motion and force control of the grasp.

6 Acknowledgements

The first author has spent a period of study within Erasmus+ program in 2015 at RWTH Aachen University that is gratefully acknowledged.

7 References

1. Rodríguez, F., Moreno, J. C., Sánchez, J. A., & Berenguel, M. (2013). Grasping in Agriculture: State-of-the-Art and Main Characteristics. In *Grasping in Robotics* (pp. 385-409). Springer London.
2. Ceccarelli, M., Figliolini, G., Ottaviano, E., Mata, A. S., & Criado, E. J. (2000). Designing a robotic gripper for harvesting horticulture products. *Robotica*, *18*(1), 105-111.
3. Li, Z. G., Liu, J. Z., & Li, P. P. (2009). Study on the collision mechanical properties of tomatoes gripped by harvesting robot. *Afr J Biotechnol*, *8*(24), 7000-7007.
4. Carbone, G., Gherman, B.G., Ceccarelli, M., Pisla, D., Itul, T.P., (2007). A robotization for packaging of horticulture products. *Robotica&Management*, 12(2), 13-20.
5. Dimeas, F., Sako, D. V., Moulianitis, V. C., & Aspragathos, N. A. (2015). Design and fuzzy control of a robotic gripper for efficient strawberry harvesting. *Robotica*, *33*(05), 1085-1098.

6. Van Henten, E. J., Hemming, J., Van Tuijl, B. A. J., Kornet, J. G., Meuleman, J., Bontsema, J., & Van Os, E. A. (2002). An autonomous robot for harvesting cucumbers in greenhouses. *Autonomous Robots*, *13*(3), 241-258.
7. Festo (2016). MultiChoiceGripper. https://www.festo.com/group/de/cms/10221.htm. Accessed 5 Mar 2016.
8. Pahl, G., & Beitz, W. (2013). *Engineering design: a systematic approach*. Springer Science & Business Media.
9. OECD (2016). Fruit and Vegetables standards. http://www.oecd.org/tad/code/. Accessed 10 Feb 2016.
10. Williams, S. H., Wright, B. W., Truong, V. D., Daubert, C. R., & Vinyard, C. J. (2005). Mechanical properties of foods used in experimental studies of primate masticatory function. *American Journal of Primatology*, *67*(3), 329-346.
11. Gładyszewska, B., & Ciupak, A. (2009). Changes in the mechanical properties of the greenhouse tomato fruit skins during storage. *PUBLISHER UWM OLSZTYN 2009*, 1.
12. Babarinsa, F. A., & Ige, M. T. (2014). Young's Modulus for Packaged Roma Tomatoes under Compressive Loading. *International Journal Of Scientific & Engineering Research*, *3*(10), 314-320.
13. Morton, M. (Ed.). (2013). *Rubber technology*. Springer Science & Business Media.
14. Ceccarelli, M. (2013). *Fundamentals of mechanics of robotic manipulation* (Vol. 27). Springer Science & Business Media.
15. Mädler (2015). MÄDLER® Katalog 41. smarthost.maedler.de/files/Katalog41_EN.zip. Accessed 12 Dec 2015.
16. Shigley, J. E. (2011). *Shigley's mechanical engineering design*. Tata McGraw-Hill Education.
17. Ceccarelli, M., Carbone, G., Cafolla, D., & Wang, M. (2016). How to use 3D printing for feasibility check of mechanism design. In *Advances in Robot Design and Intelligent Control* (pp. 307-315). Springer International Publishing.
18. Shayang Ye (2015). SHA YANG YE DC Geared Motor. http://www.shayangye.com/english/products.html. Accessed 24 Oct 2015.
19. Universal Robots (2016). Universal Robots - User Manual UR5/CB3. http://www.universal-robots.com/media/8704/ur5_user_manual_gb.pdf. Accessed 19 Jan 2016.
20. Stratasys (2015). Dimension® Elite 3D printer User Guide. http://fab.cba.mit.edu/content/tools/dimension/Dimension%20768%20Elite%20User%20Guide.pdf. Accessed 04 Jul 2015.
21. SparkFun Electronics (2016). Force Sensitive Resistor. https://www.sparkfun.com. Accessed 27 Feb 2016.
22. Arduino (2016). Arduino Nano Control Board. https://www.arduino.cc/en/Main/ArduinoBoardNano. Accessed 27 Feb 2016.
23. Robot Italy (2016). ACS712 Current Sensor. http://www.robot-italy.com. Accessed 27 Feb 2016.